C^1 Quintic Splines on Domains Enclosed by Piecewise Conics and Numerical Solution of Fully Nonlinear Elliptic Equations

Oleg Davydov* Abid Saeed†

October 11, 2016

Abstract

We introduce bivariate C^1 piecewise quintic finite element spaces for curved domains enclosed by piecewise conics satisfying homogeneous boundary conditions, construct local bases for them using Bernstein-Bézier techniques, and demonstrate the effectiveness of these finite elements for the numerical solution of the Monge-Ampère equation over curved domains by Böhmer's method.

1 Introduction

Piecewise polynomials on curved domains bounded by piecewise algebraic curves and surfaces is a promising but little studied tool for data fitting and solution of partial differential equations. Since implicit algebraic surfaces are a well-established modeling technique in CAD [6], we are interested in developing isogeometric schemes [21] for domains with such boundaries, where the geometric models of the boundary are used exactly in the form they exist in a CAD system rather than undergoing a remeshing to fit into the traditional isoparametric finite element approach.

In this paper we continue the work started in [14], where C^0 splines vanishing on a piecewise conic boundary have been introduced. In contrast to both the isoparametric curved finite elements and the isogeometric analysis of [21], our approach does not require parametric patching on curved subtriangles, and hence does not depend on the invertibility of the Jacobian matrices of the nonlinear geometry mappings. Therefore our finite elements remain piecewise polynomial everywhere in the physical domain.

This approach allows to incorporate conditions of higher smoothness in Bernstein-Bézier form standard for the theory and practice of smooth piecewise polynomials on polyhedral domains [22]. It turns out however that imposing boundary conditions make the otherwise well understood spaces of e.g. bivariate C^1 macro-elements on triangulations significantly more complex. Even in the simplest case of a polygonal domain, the dimension of the space of splines vanishing on the boundary is dependent on its

*Department of Mathematics, University of Giessen, Department of Mathematics, Arndtstrasse 2, 35392 Giessen, Germany, oleg.davydov@math.uni-giessen.de

†Department of Mathematics, Kohat University of Science and Technology, Kohat, Pakistan, abidsaeed@kust.edu.pk

geometry, with consequences for the construction of stable bases (or stable minimal determining sets) [15, 16].

In this paper we suggest a local basis defined through a minimal determining set for the space of C^1 piecewise quintic polynomials vanishing on a piecewise conic boundary and apply the resulting finite element space to the numerical solution of the fully nonlinear Monge-Ampère equation on domains with such boundary. The latter is done within the framework of Böhmer's method [7]. The results are based in part on the thesis of the second named author [26].

Böhmer's method requires stable local bases of C^1 piecewise polynomials vanishing on the boundary. In an earlier paper [16] we developed such bases on polygonal domains and demonstrated their effectiveness in solving fully nonlinear elliptic equations. Further details on Böhmer's method and references to the literature on this subject are given in Section 4.1. Note that to the best of our knowledge no method for fully nonlinear equations has been tested before on curved domains.

It is important to mention that the isoparametric approach to C^0 curved elements is problematic when finite element spaces of C^1 or higher smoothness are sought, see the remarks in [10, Section 4.7]. A successful C^1 quintic construction of this type developed in [5] seems difficult to extend to higher smoothness or higher polynomial degree. Similar difficulties to achieve C^1 or higher smoothness have recently been reported for the tensor-product based isogeometric analysis as soon as more than one patch is needed to model the geometry, see e.g. [11]. This is expected because isogeometric analysis also employs "isoparametric mappings," with tensor-product spline spaces replacing polynomials.

Remarkably, the standard Bernstein-Bézier techniques for dealing with piecewise polynomials on triangulations [22, 27] as well as recent optimal assembly algorithms [1, 2, 3] for high order elements are carried over to the spaces used here without significant loss of efficiency, see [14].

The paper is organized as follows. The spaces of C^1 piecewise polynomials on domains with piecewise conic boundary are introduced in Section 2, whereas Section 3 presents our construction of a local basis for the main space of interest $S^{1,2}_{5,0}(\triangle)$. Section 4 briefly summarizes Böhmer's method for fully nonlinear elliptic equations and presents a number of numerical experiments for the Monge-Ampère equation on smooth domains, including a circular domain, an elliptic domain, and piecewise conic domains with C^1 and C^2 boundaries.

2 C^1 piecewise polynomials on piecewise conic domains

We first recall from [14] the assumptions on a domain Ω and its triangulation $\triangle$ with curved pie-shaped triangles at the boundary.

Let $\Omega \subset \mathbb{R}^2$ be a bounded curvilinear polygonal domain with $\Gamma = \partial\Omega = \bigcup_{j=1}^{n} \overline{\Gamma}_j$, where each Γ_j is an open arc of an algebraic curve of at most second order (*i.e.*, either a straight line or a conic). For simplicity we assume that Ω is simply connected. Let $Z = \{z_1, \ldots, z_n\}$ be the set of the endpoints of all arcs numbered counter-clockwise such that z_j, z_{j+1} are the endpoints of Γ_j, $j = 1, \ldots, n$, with $z_{j+n} = z_j$. Furthermore, for each j we denote by ω_j the internal angle between the tangents τ_j^+ and τ_j^- to Γ_j and Γ_{j-1}, respectively, at z_j. We assume that $\omega_j > 0$ for all j.

Let $\triangle$ be a *triangulation* of Ω, *i.e.*, a subdivision of Ω into triangles, where each triangle $T \in \triangle$ has at most one edge replaced with a curved segment of the boundary $\partial\Omega$, and the intersection of any pair of the triangles is either a common vertex or a common (straight) edge if it is non-empty. The triangles with a curved edge are said to be *pie-shaped*. Any triangle $T \in \triangle$ that shares at least one edge with a pie-shaped triangle is called a *buffer* triangle, and the remaining triangles are *ordinary*. We denote by $\triangle_0$, $\triangle_B$ and $\triangle_P$ the sets of all ordinary, buffer and pie-shaped triangles of $\triangle$, respectively, such that $\triangle = \triangle_0 \cup \triangle_B \cup \triangle_P$ is a disjoint union, see Figure 1. Let V, E, V_I, E_I, V_B, E_B denote the set of all vertices, all edges, interior vertices, interior edges, boundary vertices and boundary edges, respectively.

For each $j = 1, \dots, n$, let $q_j \in \mathbb{P}_2$ be a polynomial such that $\Gamma_j \subset \{x \in \mathbb{R}^2 : q_j(x) = 0\}$, where $\mathbb{P}_d$ denotes the space of all bivariate polynomials of total degree at most d. By changing the sign of q_j if needed, we ensure that $\partial_{\nu_x} q_j(x) < 0$ for all x in the interior of Γ_j, where ν_x denotes the unit outer normal to the boundary at x, and $\partial_a := a \cdot \nabla$ is the directional derivative with respect to a vector a. Hence, $q_j(x)$ is positive for points in Ω near the boundary segment Γ_j. We assume that $q_j \in \mathbb{P}_1$ if Γ_j is a straight interval. Clearly, q_j is an irreducible quadratic polynomial if Γ_j is a genuine conic arc and in all cases

$$\nabla q_j(x) \neq 0 \quad \text{if} \quad x \in \Gamma_j. \tag{1}$$

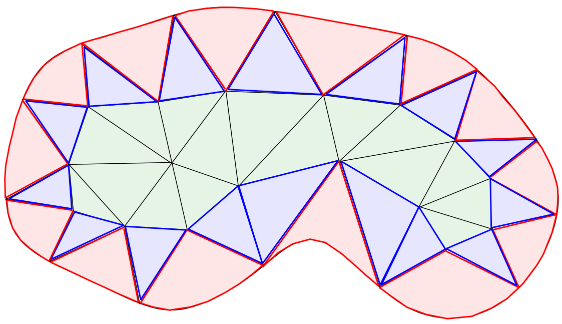

Figure 1: A triangulation of a curved domain with ordinary triangles (green), pie-shaped triangles (pink) and buffer triangles (blue).

Following [14] we assume that $\triangle$ satisfies the following conditions:

(a) $Z = \{z_1, \dots, z_n\} \subset V_B$.

(b) No interior edge has both endpoints on the boundary.

(c) No pair of pie-shaped triangles shares an edge.

(d) Every $T \in \triangle_P$ is star-shaped with respect to its interior vertex v.

(e) For any $T \in \triangle_P$ with its curved side on Γ_j, $q_j(z) > 0$ for all $z \in T \setminus \Gamma_j$.

It can be easily seen that (b) and (c) are achievable by a slight modification of a given triangulation, while (d) and (e) hold for sufficiently fine triangulations.

For any $d \geq 1$ we set

$$
\begin{aligned}
S_d^1(\triangle) &:= \{s \in C^1(\Omega) : s|_T \in \mathbb{P}_{d+i},\ T \in \triangle_i,\ i = 0,1\}, \quad \triangle_1 := \triangle_P \cup \triangle_B, \\
S_{d,I}^{1,2}(\triangle) &:= \{s \in S_d^1(\triangle) : s \text{ is twice differentiable at any } v \in V_I\}, \\
S_{d,0}^{1,2}(\triangle) &:= \{s \in S_{d,I}^{1,2}(\triangle) : s|_\Gamma = 0\}.
\end{aligned}
$$

As in [14] we use Bernstein-Bézier techniques to obtain a local basis for $S_{5,0}^{1,2}(\triangle)$ with the help of a minimal determining set.

Recall (see [22]) that the bivariate Bernstein polynomials with respect to a non-degenerate triangle $T = \langle v_1, v_2, v_3 \rangle$ with vertices $v_1, v_2, v_3 \in \mathbb{R}^2$ are defined by

$$
B_{ijk}^d(v) := \frac{d!}{i!j!k!} b_1^i b_2^j b_3^k, \quad i + j + k = d,
$$

where b_1, b_2, b_3 are the barycentric coordinates of v, that is the unique coefficients of the expansion $v = \sum_{i=1}^3 b_i v_i$ with $\sum_{i=1}^3 b_i = 1$. The Bernstein polynomials form a basis for $\mathbb{P}_d$, and the coefficients c_{ijk} in the *BB-form* expansion

$$
p = \sum_{i+j+k=d} c_{ijk} B_{ijk}^d, \quad p \in \mathbb{P}_d, \tag{2}
$$

are called the *BB-coefficients* of p. They are conveniently indexed by the elements of the set

$$
D_{d,T} := \left\{ \xi_{ijk} = \frac{iv_1 + jv_2 + kv_3}{d} \ :\ i + j + k = d,\ i, j, k \geq 0 \right\} \tag{3}
$$

of so-called *domain points*, such that $B_\xi^d := B_{ijk}^d$ and $c_\xi := c_{ijk}$ when $\xi = \xi_{ijk} \in D_{d,T}$. We will also use the notation $D_2^{d,T}(v)$ for the subset of $D_{d,T}$ consisting of the six domain points closest to a vertex v of T, in particular

$$
D_2^{d,T}(v_1) = \{\xi_{d,0,0}, \xi_{d-1,1,0}, \xi_{d-1,0,1}, \xi_{d-2,2,0}, \xi_{d-2,0,2}, \xi_{d-2,1,1}\}.
$$

The continuity and C^1-smoothness of piecewise polynomials are expressed as follows. Given two triangles $T = \langle v_1, v_2, v_3 \rangle$ and $\tilde{T} = \langle v_4, v_3, v_2 \rangle$ sharing an edge $e = \langle v_2, v_3 \rangle$, let p and $\tilde{p}$ be two polynomials of degree d written in the BB-form

$$
p = \sum_{i+j+k=d} c_{ijk} B_{ijk}^d \quad \text{and} \quad \tilde{p} = \sum_{r+s+t=d} \tilde{c}_{rst} \tilde{B}_{rst}^d,
$$

where B_{ijk}^d and $\tilde{B}_{rst}^d$ are the Bernstein polynomials with respect to T and $\tilde{T}$, respectively. Then p and $\tilde{p}$ join continuously along e if and only if their BB-coefficients over e coincide, i.e.

$$
\tilde{c}_{0jk} = c_{0kj}, \quad \text{for all } j + k = d. \tag{4}
$$

Moreover, the condition for C^1 smoothness across e is that (4) holds along with

$$
\tilde{c}_{1jk} = b_1 c_{1,k,j} + b_2 c_{0,k+1,j} + b_3 c_{0,k,j+1}, \quad j + k = d - 1, \tag{5}
$$

where (b_1, b_2, b_3) are the barycentric coordinates of v_4 relative to T.

A finite set Λ of linear functionals $\lambda : S^{1,2}_{5,0}(\triangle) \to \mathbb{R}$ is said to be a *determining set* if

$$\lambda(s) = 0 \quad \forall \lambda \in \Lambda \quad \Longrightarrow \quad s = 0,$$

and Λ is a *minimal determining set (MDS)* if there is no smaller determining set. In other words, a determining set is a spanning set of the dual space $(S^{1,2}_{5,0}(\triangle))^*$, and an MDS is a basis of $(S^{1,2}_{5,0}(\triangle))^*$. Any MDS Λ uniquely determines a *basis* $\{s_\lambda : \lambda \in \Lambda\}$ of S by duality, such that $\lambda(s_\mu) = \delta_{\lambda,\mu}$, for all $\lambda, \mu \in \Lambda$, and any spline $s \in S$ can be uniquely written in the form $s = \sum_{\lambda \in \Lambda} c_\lambda s_\lambda$, with $c_\lambda = \lambda(s) \in \mathbb{R}$.

To explain what we mean by a local basis we need some further definitions, compare [12, 14]. The *ℓ-star* of a set $A \subset \Omega$ with respect to $\triangle$ is given by

$$\mathrm{star}^1(A) = \mathrm{star}(A) := \bigcup \{T \in \triangle : T \cap A \neq \emptyset\}, \ \mathrm{star}^\ell(A) := \mathrm{star}(\mathrm{star}^{\ell-1}(A)), \ \ell \geq 2.$$

A set $\omega \subset \Omega$ is said to be a *supporting set* of a linear functional $\lambda \in (S^{1,2}_{5,0}(\triangle))^*$ if $\lambda(s) = 0$ for all $s \in S^{1,2}_{5,0}(\triangle)$ such that $s|_\omega = 0$. Given an MDS Λ, we define for each $T \in \triangle$ the set $\Lambda_T := \{\lambda \in \Lambda : T \subset \operatorname{supp} s_\lambda\}$, where $\{s_\lambda : \lambda \in \Lambda\}$ is the basis of $S^{1,2}_{5,0}(\triangle)$ dual to Λ. Thus, $\lambda \in \Lambda_T$ if and only if for a spline $s \in S$, $s|_T$ depends on the coefficient $c_\lambda = \lambda(s)$. The *covering number* κ_Λ of an MDS Λ is the maximum number of elements in Λ_T for all $T \in \triangle$.

Definition 2.1. A minimal determining set Λ for $S^{1,2}_{5,0}(\triangle)$ is said to be *ℓ-local* if there is a family of supporting sets ω_λ of $\lambda \in \Lambda$ such that $\omega_\lambda \subset \mathrm{star}^\ell(T)$ for any $T \in \triangle$ such that $\lambda \in \Lambda_T$. If Λ is *ℓ-local* for some ℓ, then the dual basis $\{s_\lambda : \lambda \in \Lambda\}$ is said to be *local.*

It is easy to check, see [14, Lemma 4.3], that if Λ is ℓ-local, then the basis functions s_λ are locally supported in the sense that $\operatorname{supp} s_\lambda \subset \mathrm{star}^{2\ell+1}(T)$ for some triangle $T \in \triangle$.

3 A local basis for $S^{1,2}_{5,0}(\triangle)$

In this section we describe a minimal determining set Λ for $S^{1,2}_{5,0}(\triangle)$, which in turn defines a basis $\{s_\lambda : \lambda \in \Lambda\}$ as explained in the previous section. For the sake of simplicity we describe the basis under the following additional assumption:

(f) All boundary edges are curved.

(g) No pair of buffer triangles shares an edge.

In fact we have implemented our bases also for the case where some boundary edges are straight. (It is used in Test Problem 4 in Section 4.3.) In this case we nevertheless assume that the triangle attached to a straight boundary edge is ordinary, and no pie-shaped triangle shares an edge with it, as in Figure 6. A description of this construction would take too much space because it has to include the handling of the boundary vertices on ordinary polygonal triangulations along the lines of [15, 16], and so we avoid this by assuming (f). Similarly, allowing buffer triangles to share edges, or equivalently, allowing more than one buffer triangle attached to a single boundary vertex would produce additional degrees of freedom on and near these edges and around the boundary vertex, also requiring the techniques of [15, 16].

We denote by V_B^1 the set of those boundary vertices $v \in V_B$ where the boundary $\partial\Omega$ has a well-defined tangent, that is either $v \notin Z$, or $\omega_j = \pi$ if $v = z_j$ for some $j = 1, \ldots, n$. In addition, $E_{P,B}$ denotes the set of all edges shared by a pie-shaped and a buffer triangle. We also set $E_I^0 := E_I \setminus E_{P,B}$.

Since splines in $S_{5,0}^{1,2}(\triangle)$ are polynomials of degree $d = 5$ on the triangles $T \in \triangle_0$, we can write these polynomials in BB-form (2),

$$s|_T = \sum_{\xi \in D_{5,T}} c_\xi B_\xi^5, \quad s \in S_{5,0}^{1,2}(\triangle). \tag{6}$$

and define for each $\xi = \xi_{ijk} \in D_{5,T}$ a functional $\lambda_\xi \in (S_{5,0}^{1,2}(\triangle))^*$ that picks the BB-coefficient c_{ijk} in (2). With the usual convention (see [22]) we identify the functional λ_ξ with the domain point ξ and speak of an MDS as a set $M \subset \overline{\Omega}$. Thanks to (4) for domain points ξ at vertices or on the edges of the subtriangulation $\triangle_0$ it does not matter which triangle in $\triangle_0$ containing ξ is used to evaluate the BB-form of a spline $s \in S_{5,0}^{1,2}(\triangle)$. The union $D_{5,\triangle_0} = \cup_{T \in \triangle_0} D_{5,T}$ forms the standard set of domain points (and corresponding functionals λ_ξ) associated with $\triangle_0$. Following the standard construction of an MDS for the space $S_5^{1,2}(\triangle_0)$ with only ordinary triangles [22], we define the following subsets of $D_{5,\triangle_0}$. For each $v \in V_I$ we choose a triangle $T_v = \langle v_1, v_2, v_3 \rangle \in \triangle_0$ attached to v, such that $v_1 = v$, and set $M_v := D_2^{5,T_v}(v) = \{\xi_{500}, \xi_{410}, \xi_{401}, \xi_{320}, \xi_{302}, \xi_{311}\} \subset D_{5,T_v}$. For each edge $e \in E_I^0$, let $T_e := \langle v_1, v_2, v_3 \rangle$ be a triangle in $\triangle_0$ attached to the edge $e = \langle v_2, v_3 \rangle$ and let $M_e := \{\xi_{122}\} \subset D_{5,T_e}$. Clearly, $\omega_\xi := T_v$ (resp. $\omega_\xi := T_e$) is a supporting set for any functional λ_ξ with $\xi \in M_v$ (resp. $\xi \in M_e$).

For each $T \in \triangle_P$, with its curved edge e given by the equation $q(x) = 0$, where $q \in \mathbb{P}_2 \backslash \mathbb{P}_1$ is irreducible and normalized so that $q(v) = 1$ for the interior vertex v of T, we notice that by Bézout theorem

$$\{s \in \mathbb{P}_6 : s|_e = 0\} = q\mathbb{P}_4 := \{qp : p \in \mathbb{P}_4\}.$$

Let T^* denote the triangle obtained by joining the boundary vertices of T by a straight line segment (see the dashed line in Figure 2). Since the Bernstein polynomials B_{ijk}^4, $i + j + k = 4$, w.r.t. T^* form a basis for $\mathbb{P}_4$ it is obvious that the set

$$\left\{qB_{ijk}^4 : i + j + k = 4\right\}$$

is a basis for $q\mathbb{P}_4$. The set of domain points of degree 4 over T^* will be denoted $D_{4,T}^*$. Even though the set $D_{4,T}^*$ formally coincides with D_{4,T^*}, the linear functionals associated with the domain points are different. Namely, each $\xi \in D_{4,T}^*$ represents a linear functional λ_ξ on $S_{5,0}^{1,2}(\triangle)$ which picks the coefficient c_ξ in the expansion

$$s|_T = q \sum_{\xi \in D_{4,T}^*} c_\xi B_\xi^4, \qquad s \in S_{5,0}^{1,2}(\triangle). \tag{7}$$

Assuming that v_1, v_2, v_3 are the vertices of a pie-shaped triangle $T \in \triangle_P$, with $v_1 \in V_I$, we set $M_T^P := \{\xi_{130}, \xi_{121}, \xi_{112}, \xi_{103}, \xi_{022}\} \subset D_{4,T}^*$, see Figure 2 where the points in M_T^P

are marked as black squares. Clearly, $\omega_\xi := T$ is a supporting set for λ_ξ. The vertices v_2, v_3 of T are shared by a pair of pie-shaped triangles and may belong to V_B^1. For each $v \in V_B^1$ let $M_v^P := \{v\} \subset D^*_{4,T_v}$, where T_v is one of the two pie-shaped triangle attached to v, and the corresponding functional is λ_v that picks the respective coefficient c_v in (7) for $T = T_v$. A supporting set for λ_v is given by $\omega_v := T_v$.

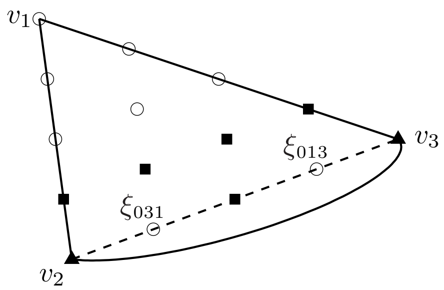

Figure 2: The set $D^*_{4,T}$ for a pie-shaped triangle T and domain points in M_T^P (black squares), and $M_{v_2}^P \cup M_{v_3}^P$ (black triangles) under the assumption that $v_2, v_3 \in V_B^1$ and $T = T_{v_2} = T_{v_3}$.

For each $T = \langle v_1, v_2, v_3\rangle$ in $\triangle_B$, where $v_1 \in V_B$, let $M_T^B := \{\xi_{411}, \xi_{222}\} \subset D_{6,T}$, see Figure 3. As usual, the functional λ_ξ identified with $\xi \in D_{6,T}$ picks the coefficient c_ξ in the BB-form expansion of $s|_T \in \mathbb{P}_6$,

$$s|_T = \sum_{\xi \in D_{6,T}} c_\xi B_\xi^6, \quad s \in S_{5,0}^{1,2}(\triangle), \tag{8}$$

and $\omega_\xi := T$ is a supporting set for any $\xi \in M_T^B$.

Remark 3.1. Let $T := \langle v_1, v_2, v_3\rangle \in \triangle_P$ with $v_1 \in V_I$. Then $s|_T = qp \in \mathbb{P}_6$ for some $p \in P_4$, where the equation $q(x) = 0$ represents the curved edge of T, with an irreducible quadratic polynomial q such that $q(v_1) = 1$. We can write all three polynomials $s|_T, q, p$ in BB-form with respect to T^*,

$$q = q_{110}B_{110}^2 + q_{101}B_{101}^2 + q_{011}B_{011}^2 + B_{200}^2 \tag{9}$$

(where we used the fact that $q(v_2) = q(v_3) = 0$),

$$s|_T = \sum_{i+j+k=6} a_{ijk}B_{ijk}^6, \quad p = \sum_{i+j+k=4} c_{ijk}B_{ijk}^4.$$

If the coefficients c_{ijk} are known, then a_{ijk} can be computed by multiplying the expansions for p and q, see the explicit formulas in [14, Eq. (35)], where a different numeration

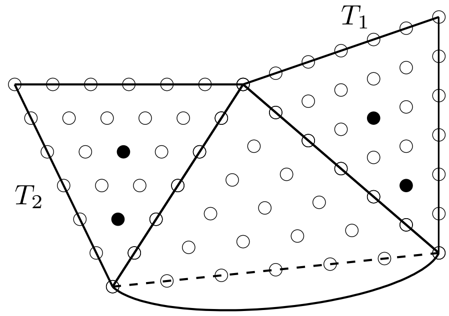

Figure 3: The domain points in the sets $M^B_{T_1}, M^B_{T_2}$ for the buffer triangles T_1, T_2 are marked with black dots.

of the vertices of T is used. Moreover, the coefficients c_{ijk} can be obtained from a_{ijk} in a stable way [14, Lemma 4.6]. To compute c_{ijk} we may write down the identity

$$\Big(\sum_{i+j+k=4} c_{ijk}B^4_{ijk}\Big)\Big(\sum_{i+j+k=2} q_{ijk}B^2_{ijk}\Big) = \sum_{i+j+k=6} a_{ijk}B^6_{ijk} \tag{10}$$

as a linear system with respect to the vector of unknown coefficients c_{ijk}, $i+j+k=4$. It is easy to check that the matrix of this system has a block structure, and by singling out the six rows of the system corresponding to the domain points in $D_2^{6,T^*}(v_1)$ we obtain a non-singular triangular linear system for the coefficients c_{ijk} corresponding to the domain points in $D_2^{4,T^*}(v_1)$, namely

$$\begin{bmatrix} 1 & 0 & 0 & 0 & 0 & 0 \\ \frac{1}{3}q_{110} & \frac{8}{15} & 0 & 0 & 0 & 0 \\ \frac{1}{3}q_{101} & 0 & \frac{8}{15} & 0 & 0 & 0 \\ 0 & \frac{1}{5}q_{110} & 0 & \frac{2}{5} & 0 & 0 \\ \frac{1}{15}q_{011} & \frac{2}{15}q_{101} & \frac{2}{15}q_{110} & 0 & \frac{4}{15} & 0 \\ 0 & 0 & \frac{1}{5}q_{101} & 0 & 0 & \frac{2}{5} \end{bmatrix} \cdot \begin{bmatrix} c_{400} \\ c_{310} \\ c_{301} \\ c_{220} \\ c_{211} \\ c_{202} \end{bmatrix} = \begin{bmatrix} a_{600} \\ a_{510} \\ a_{501} \\ a_{420} \\ a_{411} \\ a_{402} \end{bmatrix}.$$

Thus, we can compute the BB-coefficients $\{c_\xi : \xi \in D_2^{4,T^*}(v_1)\}$ of p by using only the BB-coefficients $\{a_\xi : \xi \in D_2^{6,T^*}(v_1)\}$ of $s|_T$.

Theorem 3.2. *The set*

$$M := \bigcup_{v\in V_I} M_v \cup \bigcup_{e\in E_I^0} M_e \cup \bigcup_{v\in V_B^1} M_v^P \cup \bigcup_{T\in\triangle_P} M_T^P \cup \bigcup_{T\in\triangle_B} M_T^B \tag{11}$$

is a 1-local minimal determining set for the space $S^{1,2}_{5,0}(\triangle)$.

Proof. Following the standard scheme [22] we assign some arbitrary values $c_\xi \in \mathbb{R}$ to $\lambda_\xi(s)$, for all $\xi \in M$, and show that all other coefficients c_ξ of $s \in S^{1,2}_{5,0}(\triangle)$ on all triangles

$T \in \triangle$ in the form (6), (7) or (8) depending on the type of T, can be determined from them consistently. The success of this process will show that M is an MDS. In the same time we will keep track how far the influence of a coefficient c_ξ for any $\xi \in M$ extends, to check the locality of this MDS.

It is easy to see that the set

$$M_0 := \bigcup_{v \in V_I} M_v \cup \bigcup_{e \in E_I^0} M_e$$

is a 1-local MDS for the Argyris finite element space

$$S_d^{1,2}(\triangle_0) := \{s \in S_d^1(\triangle_0) : s \text{ is twice differentiable at any vertex } v \text{ of } \triangle_0\}$$

as shown in [22, Theorem 6.1].

Let $v \in V_I$ be shared by some pie-shaped triangle $T \in \triangle_P$. Then there are also two buffer triangles $T_1, T_2 \in \triangle_B$ attached to v, see Figures 1 and 3. We know that $M_v = D_2^{5,T_v}(v) \subset D_{5,T_v}$ for some $T_v \in \triangle_0$. By [22, Lemma 5.10] and the degree raising formulas of [22, Theorem 2.39], M_v consistently determines the BB-coefficients of $s|_{T \cup T_1 \cup T_2}$ in $D_2^{6,T^*}(v) \cup D_2^{6,T_1}(v) \cup D_2^{6,T_2}(v)$. For the pie-shaped triangle T we need to go one more step and compute the BB-coefficients in $D_2^{4,T^*}(v)$ of the polynomial $p \in \mathbb{P}_4$ such that $s|_T = pq$, where the equation $q(x) = 0$ represents the curved edge of T. This can be done uniquely by solving the triangular linear system described in Remark 3.1.

Let $e = \langle v_2, v_3 \rangle \in E_I^0$ be shared by an ordinary triangle $T_e := \langle v_1, v_2, v_3 \rangle \in \triangle_0$ and a buffer triangle $T = \langle v_4, v_3, v_2 \rangle \in \triangle_B$. Assuming that the BB-coefficients of $s|_{T_e}$ for all domain points in D_{5,T_e} have been computed as described above, we can use degree raising to write $s|_{T_e}$ as a polynomial of degree six, and obtain its BB-coefficients for all domain points in D_{6,T_e}. By using the continuity and C^1 smoothness conditions (4), (5) we can then compute the BB-coefficients of $s|_T$ for all those domain points ξ_{ijk} in $D_{6,T}$, for which $i \in \{0, 1\}$. Some of them have already been computed at the previous step, namely those that belong to $D_2^{6,T}(v_2) \cup D_2^{6,T}(v_3)$. It is known that no inconsistencies arise this way, see for example the proof of [22, Theorem 6.1]. We thus obtain three new BB-coefficients of $s|_T$ corresponding to the domain points $\xi_{033}, \xi_{132}, \xi_{123} \in D_{6,T}$.

Let $v \in V_B$ and let $T_1, T_2 \in \triangle_P$ be the two pie-shaped triangles attached to v, with the curved edges given by $q_1(x) = 0$ and $q_2(x) = 0$, respectively. Let $p_1, p_2 \in \mathbb{P}_4$ be such that $s|_{T_i} = p_i q_i$, $i = 1, 2$. Since s is continuously differentiable at v and $q_1(v) = q_2(v) = 0$, we have $\nabla s(v) = p_1(v) \nabla q_1(v) = p_2(v) \nabla q_2(v)$. If $v \in V_B \setminus V_B^1$, then the vectors $\nabla q_1(v)$ and $\nabla q_2(v)$ are linearly independent, and it follows that $p_1(v) = p_2(v) = 0$, that is $c_v = 0$ in (7) for both T_1 and T_2. We now assume that $v \in V_B^1$. Then $\nabla q_1(v) = \alpha \nabla q_2(v)$ for some real $\alpha \neq 0$, which implies $p_2(v) = \alpha p_1(v)$. Let $T_1 = T_v$ be the triangle in the definition of M_v^P, in particular the functional λ_v is evaluated as $\lambda_v(s) = p_1(v)$. Thus, the value c_v in (7) for $T = T_1$ is known because M_v^P is part of the MDS M, and the value of the BB-coefficient of p_2 at the same point v is αc_v. To compute α, we just need to compare the components of the vectors $\nabla q_1(v)$ and $\nabla q_2(v)$, which is easy to do by using the BB-forms (9) of q_1, q_2 with respect to T_1^*, T_2^*, respectively.

Let $T_1 = \langle v_1, v_2, v_3 \rangle \in \triangle_B$ with $v_1 \in V_B$ and $e = \langle v_1, v_3 \rangle \in E_{P,B}$, and let $T_2 := \langle v_3, v_4, v_1 \rangle \in \triangle_P$ share the edge e with T and has its curved edge defined by the equation

$q(x) = 0$. Let us write the polynomials $s|_{T_1}$, $s|_{T_2}$ and $p \in \mathbb{P}_4$ in $s|_{T_2} = pq$ in the BB-form as

$$s|_{T_1} = \sum_{\xi \in D_{6,T_1}} \tilde{c}_\xi B^6_\xi, \quad s|_{T_2} = \sum_{\xi \in D^*_{6,T_2}} a_\xi B^6_\xi, \quad p = \sum_{\xi \in D^*_{4,T_2}} c_\xi B^4_\xi.$$

Since the domain point $\xi_{103} \in D^*_{4,T_2}$ belongs to $M^P_{T_2}$ and the coefficients c_ξ for all other $\xi \in D^*_{4,T_2} \cap e$ have been determined above, $s|_e$ is completely determined, and the BB-coefficients a_ξ for all $\xi \in D_{6,T_2} \cap e$ can be found by the multiplication of $p|_e$ by $q|_e$. Hence the smoothness conditions (4) and (5) across e give us in particular the equation

$$\begin{aligned} a_{114} &= b_1 \tilde{c}_{501} + b_2 \tilde{c}_{411} + b_3 \tilde{c}_{402} \\ &= b_1 a_{105} + b_2 \tilde{c}_{411} + b_3 a_{204}, \end{aligned}$$

where (b_1, b_2, b_3) are the barycentric coordinates of v_4 w.r.t. T_1, which determines a_{114} since $\xi_{411} \in D_{6,T_1}$ belongs to $M^B_{T_1}$. Moreover, comparing the coefficients of B^6_{114} on both sides of (10) leads to the equation

$$15 a_{114} = q_{110} c_{004} + 4 q_{101} c_{013} + 4 q_{011} c_{103},$$

and hence c_{013} can be computed from the already known BB-coefficients as

$$c_{013} = \tfrac{1}{4 q_{101}} \big(15 a_{114} - q_{110} c_{004} - 4 q_{011} c_{103} \big).$$

Note that $q_{101} \neq 0$ thanks to (1). Similarly, c_{031} is computed using the same arguments involving the buffer triangle attached to v_4. This completes the computation of the BB-form of p. By multiplying it with q we get the missing coefficients of the BB-form of $s|_{T_2}$, and by the smoothness conditions across e the BB-coefficients $\tilde{c}_{312}$ and $\tilde{c}_{213}$ of $s|_{T_1}$. The remaining unset BB-coefficients of $s|_{T_1}$ are obtained in the same way by using the pie-shaped triangle sharing the edge $\langle v_1, v_2 \rangle$ with T_1.

A close inspection of the above arguments shows that M is 1-local in the sense of Definition 2.1. ■

An example of the MDS of Theorem 3.2 for the space $S^{1,2}_{5,0}(\triangle)$ over a triangulation of a circular domain is depicted in Figure 4, where the points in the sets $\bigcup_{v \in V_I} M_v$, $\bigcup_{e \in E^0_I} M_e$, $\bigcup_{v \in V^1_B} M^P_v$, $\bigcup_{T \in \triangle_P} M^P_T$ and $\bigcup_{T \in \triangle_B} M^B_T$ are marked as black dots, diamonds, triangles, squares and downward pointing triangles, respectively. Note that $V^1_B = V_B$ in this example.

4 Numerical solution of fully nonlinear elliptic equations

To evaluate the performance of our construction of C^1 elements for curved domains we implemented Böhmer's method for fully nonlinear equations using $S^{1,2}_{5,0}(\triangle)$ as the finite element approximation space.

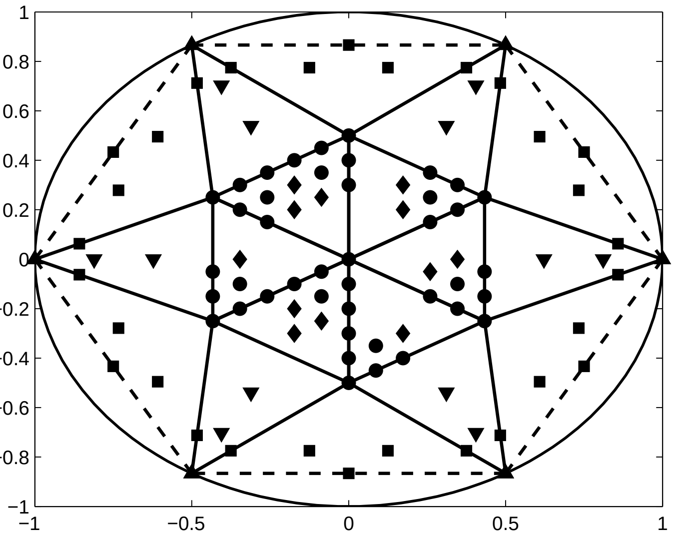

Figure 4: Example of the MDS of Theorem 3.2 for the space $S^{1,2}_{5,0}(\triangle)$ over a triangulation of a circular domain Ω.

4.1 Böhmer's method

We consider the Dirichlet problem,

$$\text{find } u : \Omega \to \mathbb{R} \text{ such that } G(u) = 0 \text{ and } u|_{\partial\Omega} = \phi, \tag{12}$$

for a second order differential operator of the form $G(u) = \widetilde{G}(\cdot, u, \nabla u, \nabla^2 u)$, where $\widetilde{G} = \widetilde{G}(w)$, $w = (x, z, p, r) \in \mathbb{R} \times \mathbb{R} \times \mathbb{R}^2 \times \mathbb{R}^{2\times 2}$ is a real valued function defined on a domain $\widetilde{\Omega} \times \Gamma$ such that $\overline{\Omega} \subset \widetilde{\Omega} \subset \mathbb{R}^2$ and $\Gamma \subset \mathbb{R} \times \mathbb{R}^2 \times \mathbb{R}^{2\times 2}$, where $\nabla u, \nabla^2 u$ denote the gradient and the Hessian of u, respectively. The operator G is said to be *elliptic* in a subset $\widetilde{\Gamma} \subset \widetilde{\Omega} \times \Gamma$ if the matrix $[\frac{\partial \widetilde{G}}{\partial r_{ij}}(w)]^2_{i,j=1}$ is well defined and positive definite for all $w \in \widetilde{\Gamma}$ [8, 20]. Under certain assumptions, including the exterior sphere condition for $\partial\Omega$, the continuity of $\phi : \partial\Omega \to \mathbb{R}$ and sufficient smoothness of $\widetilde{G}$, the problem (12) has a unique solution $u \in C^2(\Omega) \cap C(\overline{\Omega})$ if $\widetilde{\Gamma} = \widetilde{\Omega} \times \Gamma$ [20, Theorem 17.17].

The most famous example of a fully nonlinear elliptic operator which is neither quasilinear nor semilinear [8, p. 80] is the *Monge-Ampère operator* $G(u) := \det(\nabla^2 u) - g$, where $g : \Omega \to \mathbb{R}$ satisfies $g(x) > 0$ for all $x \in \Omega$. In this case $\widetilde{\Gamma} = \widetilde{\Omega} \times \mathbb{R} \times \mathbb{R}^2 \times \{r \in \mathbb{R}^{2\times 2} : r \text{ is positive definite}\}$. Under the assumptions that $\partial\Omega$ is C^3 and $g \in C^2(\overline{\Omega})$ there exists a unique *convex* solution u of (12) such that $u \in C^{2,\alpha}(\overline{\Omega})$ for all $\alpha < 1$ [20, Theorem 17.22]. References to further results about the existence and uniqueness of the solution of (12) can be found in [8, Section 2.5.7].

Many fully nonlinear elliptic operators and corresponding equations $G(u) = 0$ are important for applications, see [8]. Several numerical methods have been proposed in the literature, in particular finite difference [18, 25] and finite element type methods [4, 7, 9, 16, 19, 23, 24]. To the best of our knowledge however, no method has been tested before on non-polygonal domains.

Finite element spaces $S_0^h \subset C^1(\overline{\Omega})$ satisfying homogenous boundary conditions on Ω, where h is the maximum diameter of the underlying partition Δ^h, can be employed in *Böhmer's method* [7, 8] for the problem (12). For a fixed $h > 0$, let $u_0^h : \Omega \to \mathbb{R}$ be an initial guess satisfying the boundary condition $u_0^h|_{\partial\Omega} = \phi$. We generate a sequence of functions $\{u_k^h\}_{k\in\mathbb{N}}$ by the Newton type method

$$u_{k+1}^h = u_k^h - u^h, \quad k = 0, 1, \ldots, \tag{13}$$

where $u^h \in S_0^h$ is the Galerkin approximation of the linear elliptic problem

$$G'(u_k^h)u = G(u_k^h), \tag{14}$$

that is $u^h \in S_0^h$ is determined by the equations

$$(G'(u_k^h)u^h, v^h)_{L^2(\Omega)} = (G(u_k^h), v^h)_{L^2(\Omega)} \quad \forall v^h \in S_0^h, \tag{15}$$

where $(\cdot,\cdot)_{L^2(\Omega)}$ denotes the usual inner product in $L^2(\Omega)$, and $G'(u_k^h)$ is the linearization of the operator G at u_k^h given by

$$G'(u_k^h)u = \frac{\partial\widetilde{G}}{\partial z}(w_k^h)u + \sum_{i=1}^{2} \frac{\partial\widetilde{G}}{\partial p_i}(w_k^h)\frac{\partial u}{\partial x_i} + \sum_{i,j=1}^{2} \frac{\partial\widetilde{G}}{\partial r_{ij}}(w_k^h)\frac{\partial^2 u}{\partial x_i x_j}, \tag{16}$$

with $w_k^h(x) := (x, u_k^h(x), \nabla u_k^h(x), \nabla^2 u_k^h(x))$, $x \in \Omega$. Clearly, (15) can be reformulated into the standard weak form of the Galerkin method: Find $u^h \in S_0^h$ such that for all $v^h \in S_0^h$,

$$\int_\Omega \nabla u^h \cdot A\nabla v^h dx + \int_\Omega v^h b \cdot \nabla u^h dx + \int_\Omega c u^h v^h dx = \int_\Omega f v^h dx, \tag{17}$$

where $A = \left[\frac{\partial\widetilde{G}}{\partial r_{ij}}(w_k^h)\right]_{i,j=1}^2$, $b = \left[\frac{\partial\widetilde{G}}{\partial p_i}(w_k^h)\right]_{i=1}^2$, $c = \frac{\partial\widetilde{G}}{\partial z}(w_k^h)$ and $f = G(u_k^h)$.

Under some additional assumptions on G, satisfied in particular by the Monge-Ampère operator, it is proved in [8, Theorem 5.2] and [7, Theorem 9.1] that u_k^h converges quadratically (as $k \to \infty$) to a unique function $\hat{u}^h$ satisfying the nonlinear equations

$$(G(\hat{u}^h), v^h)_{L^2(\Omega)} = 0 \quad \forall v^h \in S_0^h,$$

such that $\hat{u}^h - u_0^h \in S_0^h$, if the initial guess u_0^h is close enough to $\hat{u}^h$. Moreover, $\hat{u}^h$ converges to the solution u of (12) in H^2-norm as $h \to 0$ if $u \in H^r(\Omega)$ for some $r > 2$ and the spaces S_0^h possess appropriate approximation properties for functions vanishing on $\partial\Omega$. Note that suitable approximation error bounds for the spaces $S_0^h = S_{5,0}^{1,2}(\triangle)$ are under investigation [17], see also related results of [14, Section 3] for the spaces of continuous piecewise polynomials vanishing on a piecewise conic boundary. Numerical results in Section 4.3 suggest that the spaces $S_{5,0}^{1,2}(\triangle)$ possess the approximation order $\mathcal{O}(h^6)$ for smooth functions vanishing on the boundary, as expected for quintic piecewise polynomials. The stability of the MDS of Theorem 3.2 and the dual local basis, important for the approximation power of the space [13], has been addressed in [26].

Note that in the case when G is only conditionally elliptic (e.g. elliptic only for a convex u for Monge-Ampère equation) the ellipticity of the linear problem (14) is only guaranteed if u_k^h satisfies the respective side condition $(x, u(x), \nabla u(x), \nabla^2 u(x)) \in \widetilde{\Gamma}$ for all $x \in \Omega$. For the Monge-Ampère equation the side condition of convexity holds for u_k^h if its second order derivatives are sufficiently close to those of the exact solution $\hat{u}$.

4.2 Implementation issues

The standard techniques of the finite element method allow efficient computation of the solution u^h of (17) using the local basis of $S_0^h = S_{5,0}^{1,2}(\triangle)$ described in Section 3. Moreover, efficient assembly algorithms for the polynomial Bernstein-Bézier shape functions introduced in [1] can be employed in the same way as described in [14, Section 5] for the continuous polynomial finite elements on curved domains enclosed by piecewise conics. We also refer to [16] for further implementation details related to fully nonlinear equations, and to [3, Section 8] for the efficient handling of the global-local transformations in the finite element method relying on Bernstein-Bézier shape functions.

4.3 Numerical results

In the experiments we focus on the Dirichlet problem for the prototypical and best studied Monge-Ampère equation,

$$G(u) = \det(\nabla^2 u) - g = 0, \quad u|_{\partial\Omega} = \phi, \tag{18}$$

with $g(x) > 0$, $x \in \Omega$, where the solution $u : \Omega \to \mathbb{R}$ is assumed to be convex for the sake of uniqueness.

We choose a number of test problems with a curved domain Ω bounded by piecewise conics, a positive function g and $\phi = 0$. As in [14, Section 6], starting from an initial triangulation of Ω, we obtain a sequence of quasi-uniform triangulations $\triangle^h$ by uniform refinement, whereby each triangle is subdivided into four triangles by joining the midpoints of every edge. For each h, we use Böhmer's method described above, with $S_0^h = S_{5,0}^{1,2}(\triangle^h)$. To solve (17) we use the 1-local basis corresponding to the MDS M of Theorem 3.2.

We follow the suggestion of [18, Remark 2.1] to use an approximate solution of the Poisson problem

$$\Delta u = 2\sqrt{g}, \quad u|_{\partial\Omega} = \phi, \tag{19}$$

as initial guess in the iterative schemes for the Monge-Ampère equation (18). Since $\phi = 0$, we choose the initial guess u_0^h in the same space $S_{5,0}^{1,2}(\triangle^h)$ and obtain it by the standard Galerkin method. However, as in [16], we get much faster convergence of the Newton iteration (13) by a multilevel approach, where this initial guess is only used on the initial triangulation, whereas on the refined triangulations a quasi-interpolant [22, Section 5.7] of the last iterate from the previous level serves as an initial guess u_0^h. As a stopping criteria for Newton iterations (13) on each level the following condition is employed:

$$\|u_k^h - u_{k+1}^h\|_{L^2(\Omega)} < 10^{-15}. \tag{20}$$

Test Problem 1. Equation (18) in the unit disk Ω centered at the origin with g chosen such that the exact solution is $u = e^{0.5(x_1^2+x_2^2)} - e^{0.5}$.

We use the same initial triangulation of the disk as in [14, Example 2], see Figure 5 (left). The numerical results for Test Problem 1 are presented in Table 1, which shows the L^2, H^1 and H^2 norms of the error $e_\ell = u_\ell - u$ of the last iterate $u_\ell = u_m^{h_\ell}$ on level ℓ against the exact solution and the number m of iterations (13) for levels $\ell = 1, \dots, 6$, where $\ell = 1$ corresponds to the initial triangulation. In addition, the first row of the

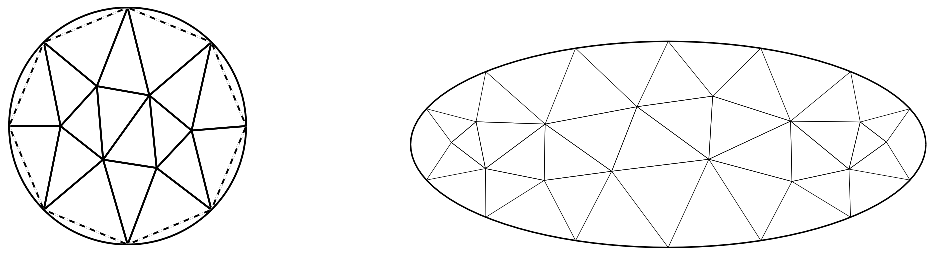

Figure 5: The domains of Test Problems 1 (left) and 2 (right), both with initial triangulations.

ℓ	L^2-error	rate	H^1-error	rate	H^2-error	rate	m
init	1.04e-2		3.20e-2		1.85e-1		
1	2.12e-6		3.84e-5		1.25e-3		2
2	2.98e-7	2.8	8.47e-6	2.2	3.35e-4	1.9	1
3	6.79e-9	5.5	3.87e-7	4.5	2.86e-5	3.6	1
4	1.36e-10	5.6	1.46e-8	4.7	2.12e-6	3.8	1
5	2.52e-12	5.8	5.23e-10	4.8	1.47e-7	3.9	1
6	9.51e-14	4.7	1.76e-11	4.9	9.53e-9	3.9	1

Table 1: Errors of the approximate solution and the rate of convergence for Test Problem 1 on the unit disk. ℓ indicates the level of refinement of the initial triangulation, and m is the number of Newton iterations (13) on the ℓ-th level. The row marked 'init' gives the errors of the initial guess on level 1.

table contains the errors of the initial guess obtained by solving (19) on the initial triangulation. The rate of convergence between levels is estimated by the usual formula $\log_2(\|e_{\ell-1}\|/\|e_\ell\|)$.

The results show the convergence rates approaching $O(h^6)$, $O(h^5)$ and $O(h^4)$ for the L^2, H^1 and H^2 norms, respectively, which is expected since the solution u is infinitely smooth and the space $S^{1,2}_{5,0}(\triangle)$ consists of piecewise polynomials of degree 5. The efficiency of the multilevel approach to the computation of the initial guesses is also confirmed since only one or two Newton iterations are needed on each level to satisfy the termination criterion (20).

Test Problem 2. Equation (18) with $g(x) = e^{x_1}$ and $\phi = 0$ in the ellipse Ω with the boundary given by the equation $x_1^2 + 6.25x_2^2 = 1$.

The initial triangulation is the same as the one used in [14, Example 1], see Figure 5 (right). The results are presented in Table 2. Since the exact solution u is not known, we use alternative measures to estimate the error. One is the residual

$$R = \|G(u_k^h)\|_{L_2(\Omega)}, \tag{21}$$

and another is the L^2, H^1 and H^2 norms of the difference $\varepsilon_\ell := u_\ell - u_{\ell+1}$ between the approximate solutions $u_\ell, u_{\ell+1}$ of two consecutive levels. Note that in the case that u_ℓ

ℓ	$\|\varepsilon_\ell\|_{L_2}$	rate	$\|\varepsilon_\ell\|_{H^1}$	rate	$\|\varepsilon_\ell\|_{H^2}$	rate	R	rate	m
init							6.58e-1		
1	1.02e-8		3.64e-7		2.90e-5		4.95e-6		4
2	9.59e-10	3.4	5.26e-8	2.8	6.37e-6	2.2	1.62e-6	1.6	1
3	1.32e-11	6.2	1.29e-9	5.3	3.16e-7	4.3	1.37e-7	3.6	1
4	2.25e-13	5.9	4.27e-11	4.9	2.05e-8	3.9	9.83e-9	3.8	1
5	8.79e-15	4.7	1.61e-12	4.7	1.56e-9	3.7	6.61e-10	3.9	1
6	—		—		—		4.33e-11	3.9	1

Table 2: Estimated errors of the approximate solution and the rate of convergence for Test Problem 2 with $g(x) = e^{x_1}$ on the ellipse. The meaning of ℓ, m and 'init' is the same as in Table 1, R is the residual error (21) for the last iterate $u_\ell = u^h_m$ on level ℓ, and $\varepsilon_\ell := u_\ell - u_{\ell+1}$ is the difference between the approximate solutions of two consecutive levels. We left the entries for $\ell = 6$ related to ε_ℓ blank because their computation requires the approximate solution u_7 of the next level.

converges to u at least linearly in some norm, we may assume that $\|u-u_{\ell+1}\| \le \gamma\|u-u_\ell\|$ for some $\gamma < 1$ if ℓ is sufficiently large. The triangle inequality then leads to $\|u - u_\ell\| \le \frac{1}{1-\gamma}\|\varepsilon_\ell\|$, so that $\log_2(\|\varepsilon_{\ell-1}\|/\|\varepsilon_\ell\|)$ may serve as an estimate of the convergence rate as long as it is positive.

We see that the numerical convergence rates in L^2, H^1 and H^2 norms are similar to those for Test Problem 1. This indicates that the solution u lies at least in $H^6(\Omega)$. In fact it is expected that u should be infinitely differentiable because so are the data and the domain boundary. Note that [20, Theorem 17.22] only assures that $u \in C^{2,\alpha}(\overline{\Omega})$ for all $0 < \alpha < 1$, but this theorem only requires C^3 boundary and C^2 smoothness of g. The convergence rate of the residual (21) is close to $O(h^4)$, that is to the rate of the H^2-norm of the error, which is plausible because R is based on the second order derivatives of the approximate solution.

Test Problem 3. Equation (18) with $g(x) = \sin(\pi|x_1|) + 1.1$ and $\phi = 0$ in the same ellipse Ω as in Test Problem 2.

The numerical results can be found in Table 3. Now [20, Theorem 17.22] is not applicable because $g \notin C^2(\overline{\Omega})$. Nevertheless, the method converges with approximate orders $O(h^{2.5})$, $O(h^{2.5})$ and $O(h^{1.5})$ for the L^2, H^1 and H^2 norms, respectively. This indicates that u should be in $H^r(\Omega)$ for $r \approx 3.5$, but the approximation order of the method in L^2 norm is suboptimal.

Test Problem 4. Equation (18) with $g(x) = 1$ and $\phi = 0$ in a C^1 domain Ω bounded by the straight lines $x_2 = \pm 1$ and semi-circles

$$x_1 = \pm\left(1 + \sqrt{1 - x_2^2}\right), \quad -1 \le x_2 \le 1.$$

The domain is shown in Figure 6 together with the initial triangulation used in our experiments. The straight line and circular segments are connected with C^1 smoothness at the points $\pm(1, 1)$ and $\pm(1, -1)$ indicated with circles.

ℓ	$\|\varepsilon_\ell\|_{L_2}$	rate	$\|\varepsilon_\ell\|_{H^1}$	rate	$\|\varepsilon_\ell\|_{H^2}$	rate	R	rate	m
init							1.06e+0		
1	2.92e-5		9.88e-4		9.48e-2		1.92e-2		3
2	5.41e-6	2.4	6.20e-5	3.9	4.44e-3	4.4	6.23e-3	1.6	2
3	1.21e-6	2.2	1.19e-5	2.4	1.40e-3	1.7	2.03e-3	1.6	1
4	6.84e-8	4.1	2.01e-6	2.6	4.90e-4	1.5	7.46e-4	1.4	1
5	1.44e-8	2.3	3.67e-7	2.5	1.47e-4	1.7	2.47e-4	1.6	1
6	—		—		—		9.04e-5	1.5	1

Table 3: Estimated errors of the approximate solution and the rate of convergence for Test Problem 3 with $g(x) = \sin(\pi|x_1|) + 1.1$ on the ellipse. The layout is the same as in Table 2.

Similar to the tests with $g(x) = 1$ on a square domain [16, Section 5.1], our experiments do not show convergence of the method with respect to ℓ. This is explained in particular by the fact that the second derivatives of the solution u of (18) with $\phi = 0$ may not be continuous along any straight line boundary segment unless g vanishes on this segment. Nevertheless, in contrast to the square domain, the approximate solutions u_ℓ keep the convex shape and the Newton iterations converge on each level. Figure 7 shows u_2 and its contour plot.

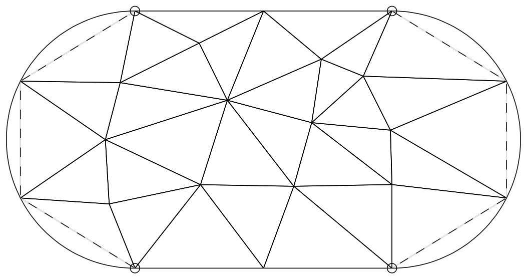

Figure 6: The domain of Test Problem 4 with initial triangulation. The boundary is C^1 at the four points marked with circles and C^∞ elsewhere. Its top and bottom pieces are straight line segments.

Test Problem 5. Equation (18) with $g(x) = 1$ and $\phi = 0$ in a centrally symmetric C^2 domain Ω bounded by two elliptic and two circular segments, see Figure 8, where the top elliptic segment is given parametrically by the equations

$$x_1 = 4\cos t,\ x_2 = 1.3\sin t - c_2, \quad 0.15\pi \le t \le 0.85\pi,$$

and the left circular segment has radius r and center $(c_1, 0)$, with r and (c_1, c_2) being the radius and the center of the osculating circle to the ellipse $x_1 = 4\cos t$, $x_2 = 1.3\sin t$ at the point defined by $t = 0.85\pi$.

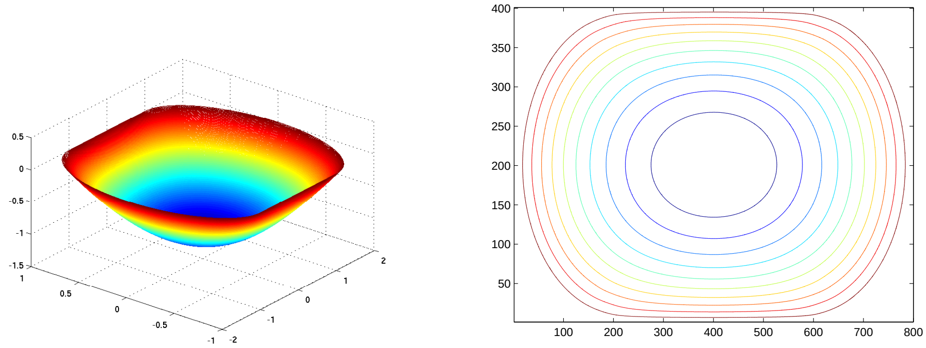

Figure 7: Approximate solution u_ℓ of Test Problem 4 for the level $\ell = 2$ and its contour plot.

It is easy to check that elliptic and circular segments of Ω join with continuous curvature. We use the initial triangulation shown in Figure 8. The numerical results presented in Table 4 indicate $O(h^4)$, $O(h^3)$ and $O(h^2)$ convergence order in the L_2, H^1 and H^2-norm, respectively, so that the solution u is expected to belong to $H^r(\Omega)$ for $r \approx 4$. Note that [20, Theorem 17.22] is not applicable because the boundary is not C^3.

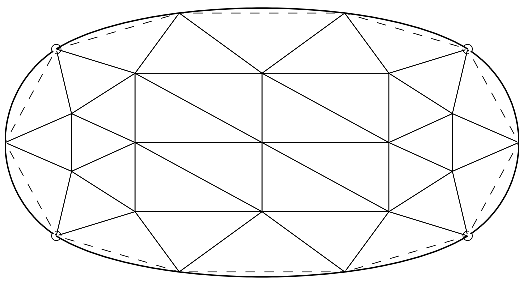

Figure 8: The domain of Test Problem 5 with initial triangulation. The boundary is C^2 at the four points marked with circles and C^∞ elsewhere.

References

[1] M. Ainsworth, G. Andriamaro and O. Davydov, Bernstein-Bézier finite elements of arbitrary order and optimal assembly procedures, SIAM J. Sci. Comp., 33 (2011), 3087–3109.

[2] M. Ainsworth, G. Andriamaro and O. Davydov, A Bernstein-Bézier basis for arbitrary order Raviart-Thomas finite elements, Constr. Approx. 41 (2015), 1–22.

ℓ	$\|\varepsilon_\ell\|_{L_2}$	rate	$\|\varepsilon_\ell\|_{H^1}$	rate	$\|\varepsilon_\ell\|_{H^2}$	rate	R	rate	m
init							2.01e+0		
1	1.07e-3		1.00e-2		1.34e-1		9.10e-2		2
2	4.87e-5	4.5	8.56e-4	3.5	2.20e-2	2.6	2.20e-2	2.0	1
3	3.04e-6	4.0	1.04e-4	3.0	5.30e-3	2.0	5.87e-3	1.9	1
4	2.09e-7	3.7	1.39e-5	2.9	1.38e-3	1.9	1.56e-3	1.9	1
5	1.58e-8	3.7	2.01e-6	2.8	3.80e-4	1.9	4.15e-4	1.9	1
6	—		—		—		1.11e-4	1.9	1

Table 4: Estimated errors of the approximate solution and the rate of convergence for Test Problem 5 on a C^2 domain. The layout is the same as in Table 2.

[3] M. Ainsworth, O. Davydov and L. L. Schumaker, Bernstein-Bézier finite elements on tetrahedral-hexahedral-pyramidal partitions, Comput. Method Appl. Mech. Engrg., 304 (2016), 140–170.

[4] G. Awanou, Pseudo transient continuation and time marching methods for Monge-Ampère type equations, Adv. Comput. Math., 41 (2015), 907–935.

[5] M. Bernadou, Curved finite elements of class C^1: Implementation and numerical experiments. Part 1: Construction and numerical tests of the interpolation properties, Comput. Method Appl. Mech. Engrg., 106(1-2) (1993), pp. 229–269.

[6] J. Bloomenthal et al, Introduction to Implicit Surfaces, Morgan-Kaufmann Publishers Inc., San Francisco, 1997.

[7] K. Böhmer, On finite element methods for fully nonlinear elliptic equations of second order, SIAM J. Numer. Anal., 46(3) (2008), 1212–1249.

[8] K. Böhmer, Numerical Methods for Nonlinear Elliptic Differential Equations: A Synopsis, Oxford University Press, Oxford, 2010.

[9] S.C. Brenner, T. Gudi, M. Neilan, L.-Y. Sung, C^0 penalty methods for the fully nonlinear Monge-Ampère equation, Math. Comput., 80(276) (2011), 1979–1995.

[10] S. C. Brenner, and L.R. Scott, The Mathematical Theory of Finite Element Methods, Springer, New York, 1994.

[11] A. Collin, G. Sangalli, T. Takacs, Analysis-suitable G^1 multi-patch parametrizations for C^1 isogeometric spaces, preprint, 2016, `arXiv:1509.0761`.

[12] O. Davydov, Stable local bases for multivariate spline spaces, J. Approx. Theory, 111 (2001), 267–297.

[13] O. Davydov, Smooth finite elements and stable splitting, Berichte "Reihe Mathematik" der Philipps-Universität Marburg, 2007-4 (2007). An adapted version has appeared as [8, Section 4.2.6].

[14] O. Davydov, G. Kostin and A. Saeed, Polynomial finite element method for domains enclosed by piecewise conics, CAGD, 45 (2016), 48–72.

[15] O. Davydov and A. Saeed, Stable splitting of bivariate spline spaces by Bernstein-Bézier methods, *in* "Curves and Surfaces - 7th International Conference, Avignon, France, June 24-30, 2010" (J.-D. Boissonnat et al, Eds.), LNCS 6920, Springer-Verlag, 2012, pp. 220–235.

[16] O. Davydov and A. Saeed, Numerical solution of fully nonlinear elliptic equations by Böhmer's method, J. Comput. Appl. Math., 254 (2013), 43–54.

[17] O. Davydov and W. P. Yeo, On the approximation power of C^1 piecewise polynomials on piecewise conic domains, in preparation.

[18] E. J. Dean and R. Glowinski, Numerical methods for fully nonlinear elliptic equations of the Monge-Ampère type, Comput. Method Appl. Mech. Engrg., 195 (2006), 1344–1386.

[19] X. Feng, M. Neilan, Mixed finite element methods for the fully nonlinear Monge-Ampère equation based on the vanishing moment method, SIAM J. Numer. Anal., 47(2) (2009) 1226–1250.

[20] D. Gilbarg and N. S. Trudinger, Elliptic Partial Differential Equations of Second Order, Springer-Verlag, Berlin, 2001.

[21] T. J. R. Hughes, J. A. Cottrel, Y. Bazilevs, Isogeometric analysis: CAD, finite elements, NURBS, exact geometry and mesh refinement, Comput. Methods Appl. Mech. Engrg., 194(2005) 4135-4195.

[22] M. J. Lai and L. L. Schumaker, Spline Functions on Triangulations, Cambridge University Press, 2007.

[23] O. Lakkis, T. Pryer, A finite element method for nonlinear elliptic problems SIAM J. Sci. Comp. 35 (2013), A2025–A2045.

[24] M. Neilan, Finite element methods for fully nonlinear second order PDEs based on a discrete Hessian with applications to the Monge-Ampère equation, J. Comput. Appl. Math. 263 (2014), 351–369.

[25] A. Oberman, Wide stencil finite difference schemes for the elliptic Monge-Ampère equations and functions of the eigenvalues of the Hessian, Discrete Contin. Dyn. Syst. Ser B 10(1) (2008), 221–238.

[26] A. Saeed, Bivariate Piecewise Polynomials on Curved Domains, with Applications to Fully Nonlinear PDE's, PhD thesis, University of Strathclyde, Glasgow, 2012.

[27] L. L. Schumaker, Spline Functions: Computational Methods, SIAM (Philadelphia), 2015.